

AN EXPERIMENTAL STUDY OF SWEEP ANGLE EFFECTS ON THE TRANSITION POINT ON A 2D WING BY USING HOT-FILM SENSOR

Soltani M.R. and Davari A.R. and Hassanzadeh khakmardani M.*, M.Masdari

*Author for correspondence
Department of Aerospace Engineering,
Sharif University of Technology
Tehran,
Iran,
E-mail: maryam_2hkh@yahoo.com

ABSTRACT

Location of transition point over a 2-D swept wing was investigated. A series of wind tunnel tests were performed to predict the transition location over three models of swept wing having same aspect ratio, and at various angles of attack and sweep angles by hot-film anemometer. Two flat plates were used at the ends of the models to prevent the flow to roll up and to reduce the boundary layer effect of the test section on the models, but the flow field on the model was still 3D because of the swept angle effects that led to formation of cross flow over the wing surface. Due to the complexity of the calibration of the hot film sensors, as well as various sources of errors in the calibration process, the hot film sensors were not calibrated and their signal is qualitatively investigated.

Data obtained from the hot film sensor signal indicates that as the swept angle increases, the position of transition moves toward the leading edge of the wing due to strengthening of the cross flow about the leading edge, and transition occurs at a smaller angle of attack. Increasing the angle of attack also moved the position of transition point closer to the leading edge of the wing. The transition line is approximately parallel to the x/c local line which may indicate that the strength of cross flow is nearly constant on each line parallel to the $c/4$ local line.

NOMENCLATURE

Λ	[-]	Sweep angle
α	[-]	Angle of attack
b	[m]	Wing span
x	[m]	Length in chordwise direction
y	[m]	Length in spanwise direction
c	[m]	Wing local chord

Subscripts

SD	Standard deviation
Sk	skewness

INTRODUCTION

Swept wings have been used in many airplanes at different flight regimes. One advantage of these wings is that they produce no significant increase in the drag force. Aerodynamic study of wings having swept angle in subsonic flow has special importance due to obligation to pass to this flow on landing and takeoff phase. Swept wing at high speed airflow has not sufficient time to react so simply and directly the flow is moving front to back over the wing, but at low speeds airflow has opportunity to react and compress in the spanwise direction by swept leading edge toward the wing tip. The airflow at the wing tips moves along the wing rather than moving over it, that will introduce spanwise flow. Lift of wing is produced by the air flow passing over it. With increase of spanwise flow, boundary layer on the wing is thicker and transition to turbulence or flow separation on the wing are more likely to happen. The aspect ratio of the wing decreases and with air leakage around the wing tip its effectiveness decreases. The spanwise flow increases toward the wing tip; therefore the lift at the wing tip drops earlier than that at the wing root.

Swept wing boundary layer has 4 major instability modes; attachment line instability, stream wise instability, spanwise instability and finally centrifugal mode. These modes, either alone or in combination, affect the transition on the swept wing. Leading edge instabilities can be controlled by controlling the radius of the leading edge. In models having the low leading edge radiuses, this mode of instability, leading edges is not dominated. Cross flow instability is the main transition mechanism for the swept wings. When the free flow get to the

leading edge streamlines bends out because of swept angle and suddenly its pressure decreases. The Streamlines then curved inward and moved along the chord wise direction to reach the lowest pressure. Finally, near the leading edge they bend in because of increasing the pressure again. Cross flow instability may appear to be stationary or traveling waves. Stationary cross flow disturbances dependence on the surface roughness and appear in the low turbulence environment. Travelling disturbances of cross flow is not associated with surface roughness, but it is influenced by the free flow turbulence and appears in the high turbulence environments.

EXPERIMENTAL APPARATUS

All experiments were conducted in a subsonic wind tunnel of closed return type with a test section size of $80 \times 80 \times 200 \text{ cm}^3$, operating at speeds ranging from 10 to 100m/s. The inlet of the tunnel has a 7:1 contraction ratio with four large anti-turbulence screens and a honeycomb in its settling chamber to reduce tunnel turbulence to less than 0.1% in the test section. The models used in these tests are the scaled models of a tapered wing whose sections similar to the NACA 6 series airfoils (see figure1). A half model is designed and fabricated to achieve higher Reynolds numbers during the tests. Two flat plates are used at the tip and root of the models to reduce the boundary layer effect of the test section and trailing edge vortices on the models. The baseline configuration is a semi- span, 1:2.5 scale model of the actual wing. The models have different sweep angles of 23, 33 and 40 degree with the same aspect ratio and a span of 516 mm (see figure 2).

For experimental study of boundary layer transition, ten hot film sensors were used. The hot film system used constant temperature hot film anemometer. The frequency modulation for recording hot film data had a frequency response of 10 KHz. The hot film sensors were mounted with 30 degree relative to each other to prevent their wake effects on each other (see figure3).

RESULTS AND DISCUSSION

Duo to interference effects of sweep angle, stream wise and spanwise instabilities, and interference effects related to three dimensional flows on the wing not can be used a general process to determine the position of transition. The sudden increase in voltage level that is associated with increased

fluctuation could represent the beginning or the occurrence of transition. Voltage level in turbulent flow reduced relatively in compared with the transition mode. but duo to the random nature of turbulent flow that tends to happen random phenomenon, any random phenomenon that occur in flow such as formation of travelling vortices or breaking them into small vortices, can increase the amount of fluctuation in the signal received from a hot film sensors. By qualitative study of voltage versus time the point of transition can be roughly estimated. Increasing the voltage level associated with the hot film sensor performance represents an increase in the velocity and heat transfer rate in flow. Since here not calibrated hot film sensors, for proper comparison between data, graphs are drown in such a way that the hot film sensor signals at different locations and different angles of attack could be compared with each other.

Error sources involve the error of the sensors and the error due to the measurement method. Error of measurement method is not important because data analyses are qualitative, sensors are not calibrated.

To confirm the diagnosis of transition location of boundary layer at different angles of attack, statistical information output from the hot film sensors are also to be used.

- Standard deviation: represents diffusion of values around the mean value.
- Skewness: represents the asymmetry of the potential distribution.

For a perfectly symmetrical distribution, the value of skewness is zero. For an asymmetric distribution elongated toward higher values skewness is positive, and for asymmetric distribution elongated toward small amounts skewness is negative.

For each of the analysis, in this paper, only the data of a few sensors are analyzed. The sensors are selected in such a way the various effects such as wing swept angle, angle of attack, etc. can be distinguished. As the top of each graph, a schematic of the wing along with location of ten sensors are showed. The sensor under consideration is the one with dark circle.

From Fig.4 it can be seen that with increasing the angle of attack, voltage level and fluctuation of the S1 sensor, dark circle, shown on the wing surface at the top of Fig.4a, gradually increase up to 4 degrees angle of attack.

With increasing angle of attack to 5 degree, voltage level almost remained constant. Fluctuation level has been increased significantly at 6 degree angle of attack that is an indication of the transition onset in the flow. At 7 and 8 degree angles of attack with increasing the fluctuation and dropping the output voltage, the turbulent flow seems to be fully established, Fig. 4a.

A remarkable difference in voltage level between angles of attack -2, 0 and 2 degree, can be observed in this figure, Fig.4a. This difference in the voltage level gradually decreases with increasing the angle of attack. Sensor 5 is located at a farther position relative to wing leading edge (see figure 5).

The sudden increase in the voltage level between angles of attack of -2 and 0 degrees is not evident. Cross flow at the leading edge has the highest strength and as moving it towards the trailing edge, the cross flow strength decreases. Effect of cross flow at -2 degree angle of attack is dominant. This sudden increase in the voltage level from -2 to 0 degrees angles of attack which gradually decreases with increasing the angle of attack can be attributed to the strengthening of cross flow mode.

From figures 5 it is seen that for the S5 sensor at 1 degree angle of attack, voltage level and fluctuation has been increased which may indicate the occurrence of transition. Occurrence of transition at lower angle of attack is logical because the sensor is located far away from the leading edge. Thus comparing figures 4a and 5a, with increasing the angle of attack transition position occurs closer to the leading edge of the wing.

Figures 6a Shows that by increasing the angle of attack fluctuation gradually increases and the transition occurs at 6 degree angle of attack for sensor 6, the S6. Comparing figures 4a and 6a similar trend is observed, because both sensors are almost located at a same location relative to the local chord, near the leading edge.

Cross flow strength almost remains constant during the local chord line. It can cause the same transition line within the local chord of the wing. On the chart of sensor 6, Fig. 6a, a voltage level difference between -2 degree angle of attack and positive angles is evident, that can associated with the dominance of the cross flow mode at -2 degree angle of attack.

Data of sensor 1 for the swept angle of 33 degree is shown in figure 7. It is seen that by away from the leading edge an increase in the voltage level between

-2 degree angle of attack and positive angles is not apparent. It can be seen that the fluctuation of -2, 0 and 2 degree angles of attack is almost constant and with increasing the angle of attack to 5 degrees, the fluctuation increases. Thus the 5 degrees angle of attack the flow transition is observed to be initiated. At 8 degree angle of attack voltage level slightly reduces that shows turbulence in the flow, figure 7a-c.

For the largest wing swept angle, $\Lambda = 40^\circ$, the data of sensor number 1 is analysed, figure 8. It is seen that for this sensor the voltage level gradually increased with increasing the angle of attack, but at 4 degrees angle of attack a sudden rise in the voltage level and in the fluctuation is occurred. Between 4 to 6 degrees angles of attack the voltage gradually increases with increasing the angle of attack and at 7 degrees angle of attack the voltage remains almost constant. Thus at 4 degrees angle of attack can be considered as the transition angle of attack for his wing at this situation. Voltage level slightly decreases by increasing angle of attack to 8 degree that can be shown flow transition. The striking differences in the voltage level between positive and negative angles of attack can be linked to the dominant cross flow mode at negative angles where the strength of this mode gradually decreases with increasing angle of attack to positive ones.

Comparing figures 4a, 7a and 8a it can be seen that all of the cases have same location relative to the leading edge. It further can be seen that the transition for wings with 23, 33 and 40 sweep angles occurs respectively at angles of attack of 6, 5, 4 degrees. It shows that increasing the sweep angle reduces the angle of attack at which transition occurs. This is due to the dimensional effects of the flow.

CONCLUSION

Experiments were conducted to study qualitative analysis of the transition phenomenon and the effects of swept angle and angle of attack on its location. Tests were conducted at a constant speed 50 m/s and on that range between -2 to 0 degrees angles of attack. The angle of attack range was chosen such that the cross flow strength at different conditions could be examined.

The following results include the effects of sweep angle and angle of attack on the transition location of the two dimensional swept wing.

Effect of angle of attack- Generally by increasing the angle of attack, position of sensor which sense the

transition is close to the leading edge of the wing and flow in a shorter distance from the leading edge remains laminar. For sensors farther from the leading edge of the wing transition occurs at lower angle of attack and for sensors close to the leading edge transition occurs at higher angle of attack.

Effect of sweep angle- At the same positions, by increasing the sweep angle transition occurs at lower angles of attack i.e. the transition to turbulent is hastened. This is more prominent at the locations close to the leading edge since with increasing the sweep angle the strength of the cross flow on the wing increases. After the leading edge the cross flow has its maximum strength and as moving towards the trailing edge, its strength decreases.

Effect of cross flow- At fixed longitudinal position in two sections one near the tip of wing and the other one near the root of wing, transition will occur relatively at the same angle of attack owing to the equal cross flow strength.

Interaction of angle of attack and sweep angle- by increasing sweep angle at a fixed angle of attack transition can be occurred rapidly. Also at a fixed x/c , as increasing the wing sweep angle, the angle of attack in which, the transition occurs, decreases.

REFERENCES

- [1] Harry R.Chiles, The Design and Use of a Temperature-Compensated Hot-Film Anemometer System For Boundary-Layer Flow Transition Detection On Supersonic Aircraft, NASA Technical Memorandum No 100421,1988
- [2] Saric,W.S., Low-Speed Boundary-Layer Transition Experiments, Draft Copy, Mechanical and Aerospace Engineering, Arizona State University, 1994.
- [3] Carr, L.W., Cebeci, T., Boundary Layers on Oscillating Airfoil, 1985
- [4] Knapp,C.F., and Roache, P.J., A Combined Visual and Hot-Wire Anemometer Investigation of Boundary-Layer Transition. AIAA Journal, Vol. 6, No. 1, 1968, PP. 29-36.
- [5] Reda,H.L., Boundary Layer Stability and Transition, FED, Vol.114, 1989.
- [6] Saric, W.S., Low-Speed Boundary-Layer Transition Experiments, Draft Copy, Mechanical and Aerospace Engineering, Arizona State University, 1994.
- [7] R.A.Rozendaal, Natural Laminar Flow Flight Experiments on a Swept Business Jet-Boundary Layer Stability Analyses, NASA Contractor Report 3975, 1986.
- [8] R.A.Rozendaal, Natural Laminar Flow Flight Experiments on a Swept Business Jet-Boundary Layer Stability Analyses, NASA Contractor Report 3975, 1986.
- [9] D.V.Maddalon and F.S.collier, Jr and L.C.Montoya and R.J.Putnam, Transition Flight Experiments on a Swept Wing with

Suction, Presented at the IUTAM Third Symposium on Laminar-Turbulent Transition, Toulouse, France, September 11-5, 1989.

- [10] J.Ray Dagenhart, Cross flow Stability And Transition Experiments in a Swept-Wing Flow, NASA Technical Memorandum 108650, 1992.

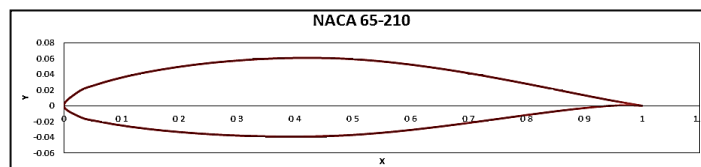


Figure 1- Wing section airfoil

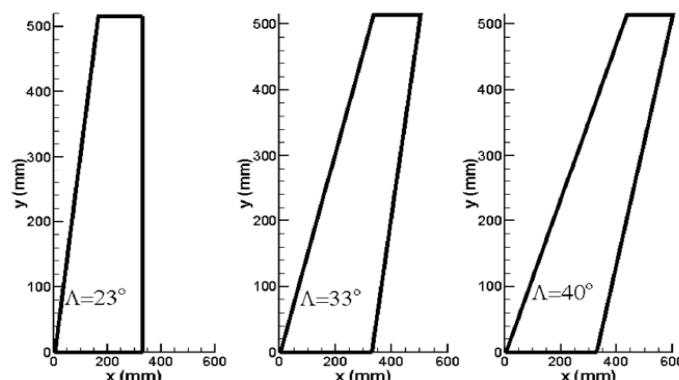
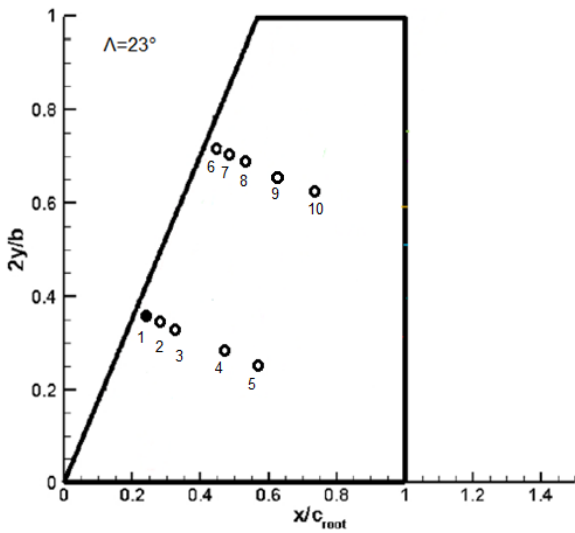


Figure 2- Three half models with 23, 33 and 40 degree swept angles



Figure 3- The model with hot film sensors in the test section



$\Lambda = 23^\circ, S1$

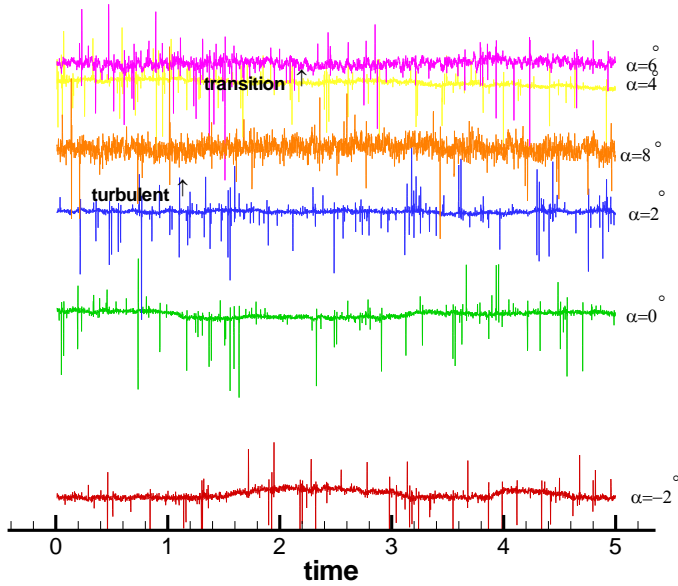


Figure 4a- Voltage-time graph, $x/c=0.03$, $2y/b=0.36$, $\Lambda = 23^\circ$

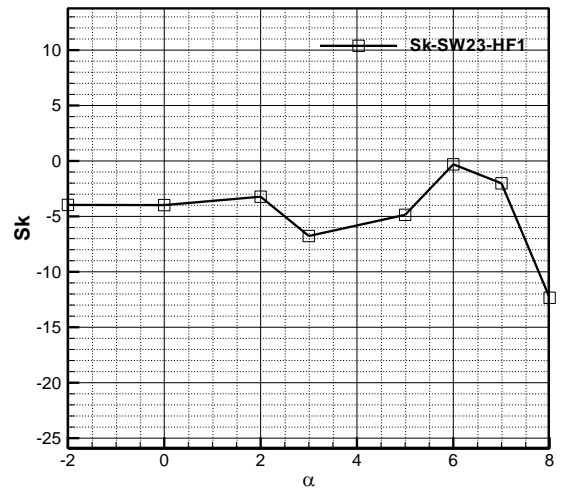


Figure 4b- Skewness graph, $x/c = 0.03$, $2y/b = 0.36$, $\Lambda = 23^\circ$

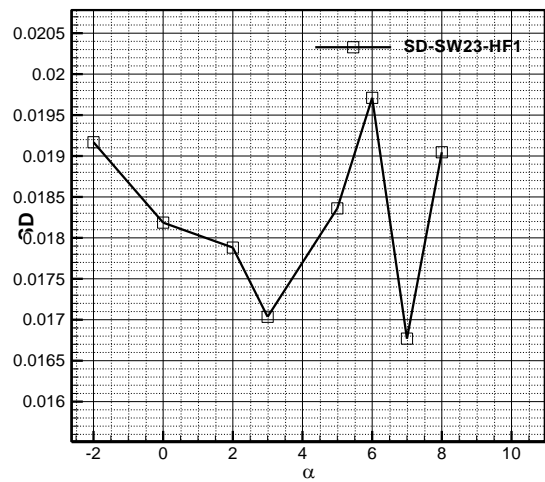
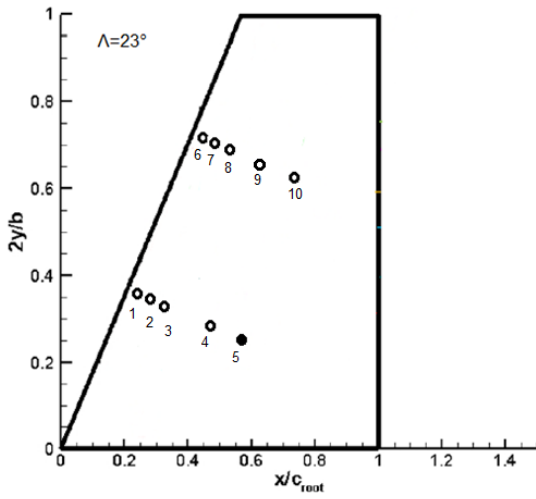


Figure 4c- Standard deviation graph, $x/c=0.03$, $2y/b=0.36$, $\Lambda = 23^\circ$



$\Lambda = 23^\circ, S5$

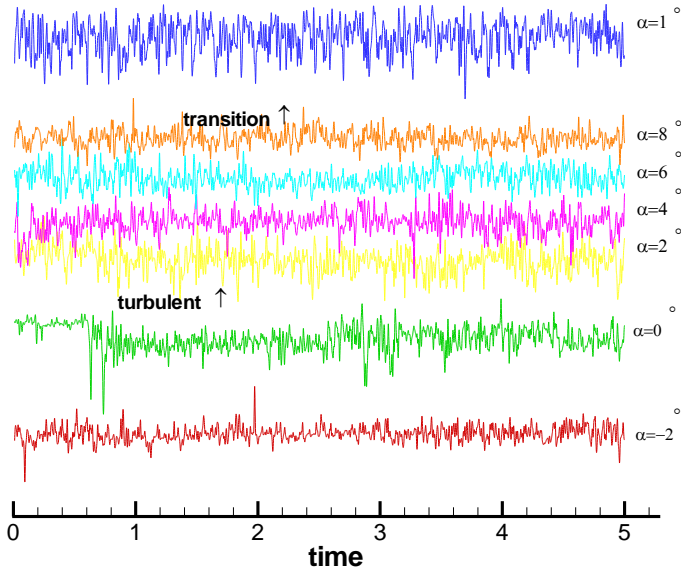


Figure 5a- Voltage-time graph, $x/c=0.49$, $2y/b = 0.25$, $\Lambda = 23^\circ$

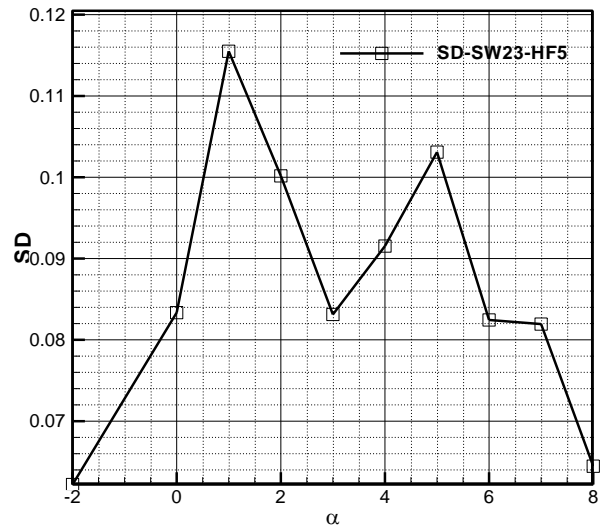


Figure 5b- Standard deviation graph, $x/c = 0.49$, $2y/b = 0.25$, sweep angle = 23 degree

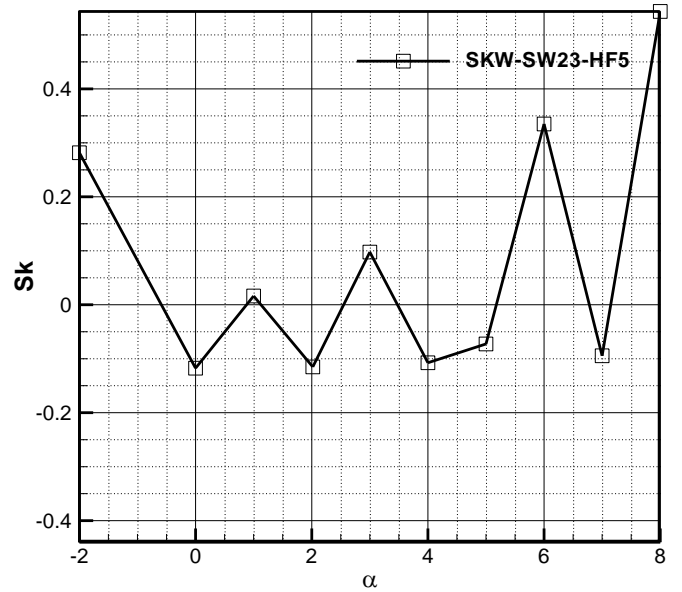


Figure 5c- Skewness graph, $x/c = 0.49$, $2y/b = 0.25$, $\Lambda = 23^\circ$

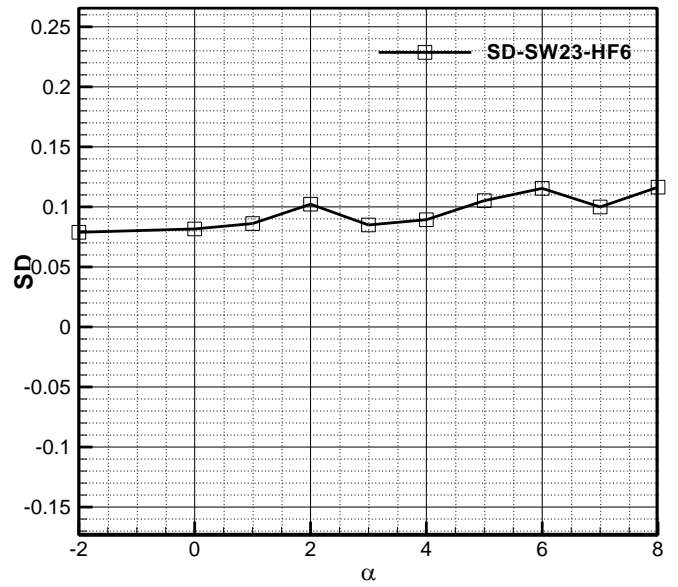
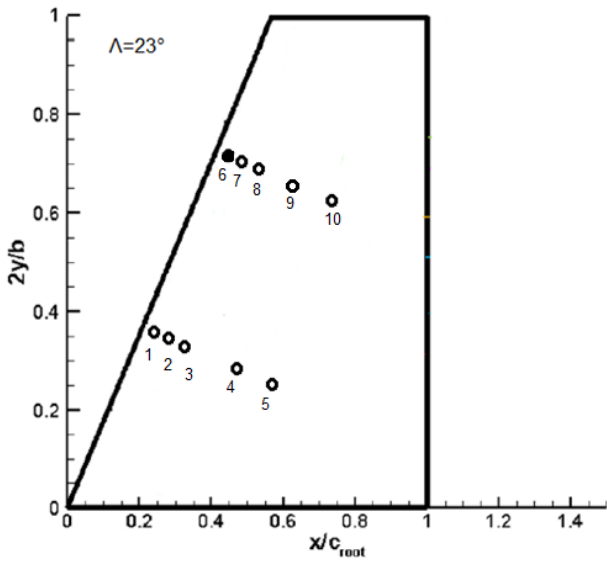


Figure 6b- Standard deviation graph, $x/c=0.04$, $2y/b=0.71$, sweep angle = 23 degree

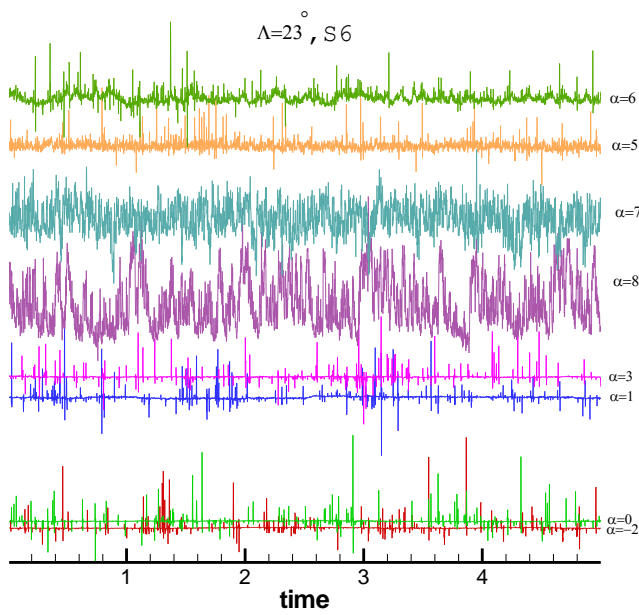


Figure 6a- Voltage-time graph, $x/c=0.04$, $2y/b=0.71$, $\Lambda=23^\circ$

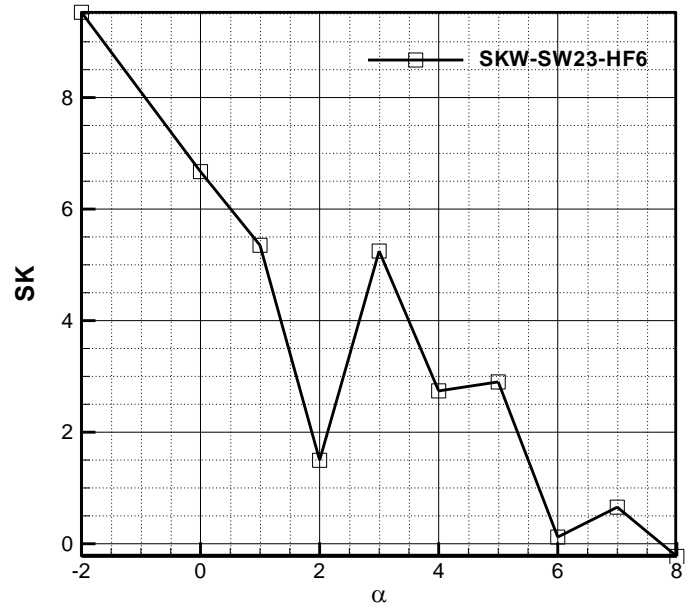


Figure 6c- Skewness graph, $x/c=0.04$, $2y/b=0.71$, $\Lambda=23^\circ$

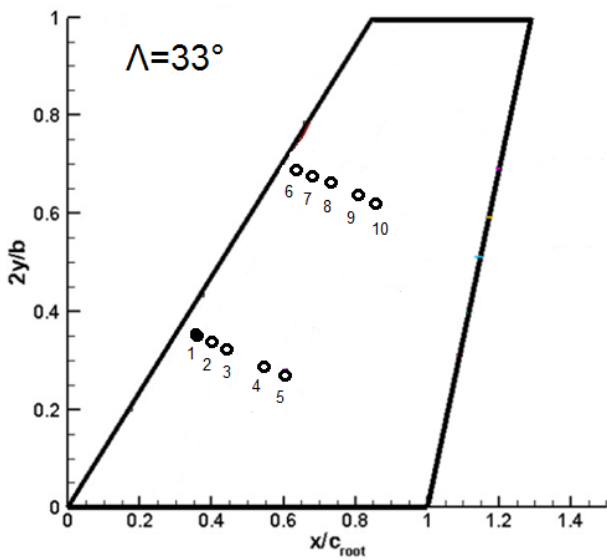


Figure 7a- Voltage-time graph $x/c=06, 2y/b=0.03,$
 $\Lambda = 23^\circ$

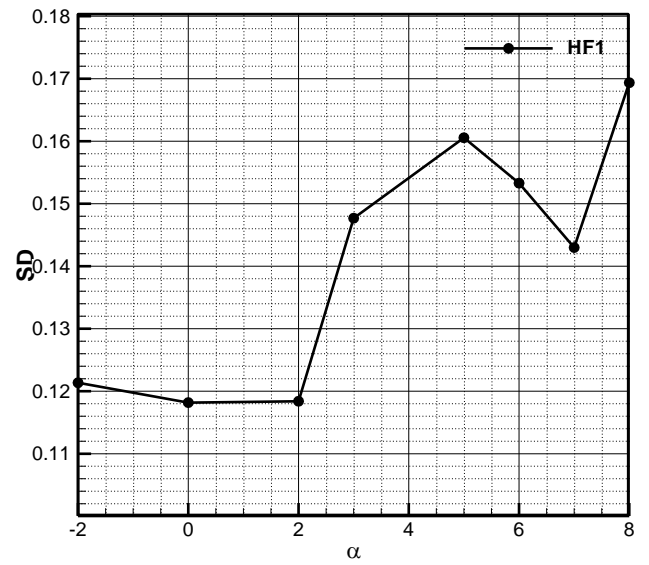


Figure 7b- Standard deviation graph $x/c =06,$
 $2y/b=0.03, \Lambda =23^\circ$

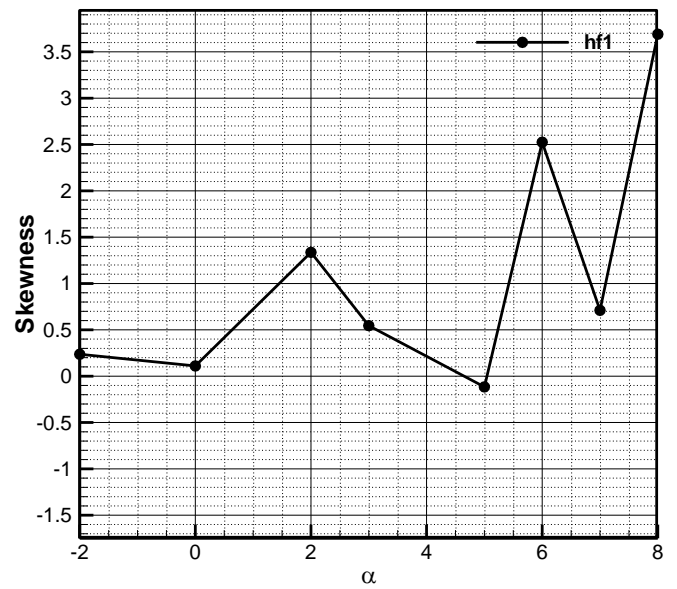


Figure 7c- Skewness graph $x/c =06, 2y/b=0.03, \Lambda =23^\circ$

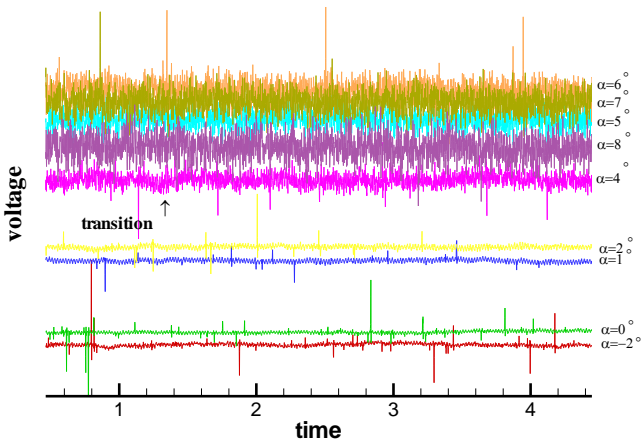
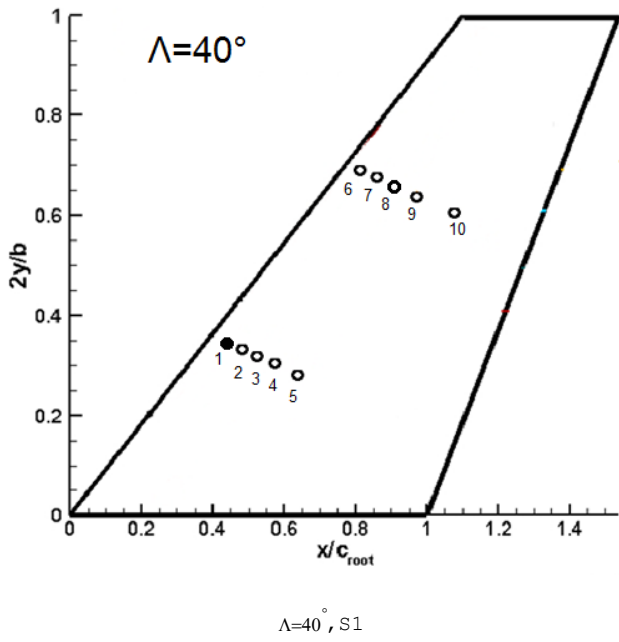


Figure 8a- Voltage-time graph $x/c=0.63$, $2y/b=0.34$, $\Lambda = 23^\circ$

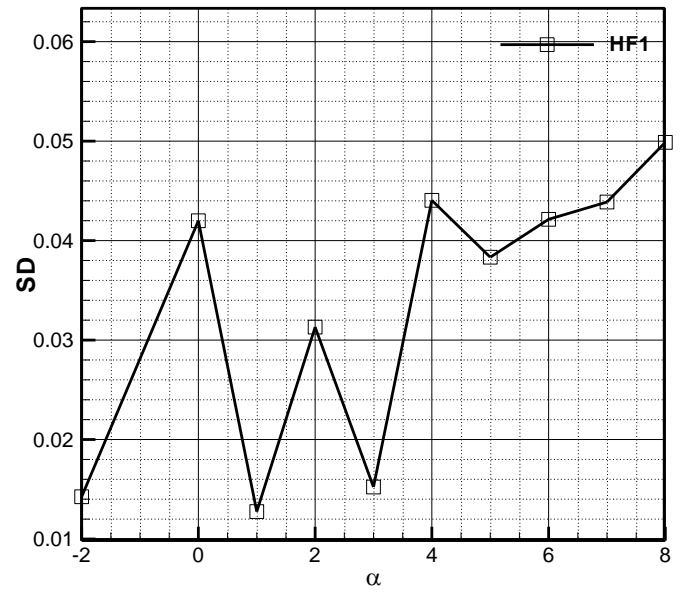


Figure 8b- Standard deviation graph $x/c=0.63$, $2y/b=0.34$, $\Lambda = 23^\circ$

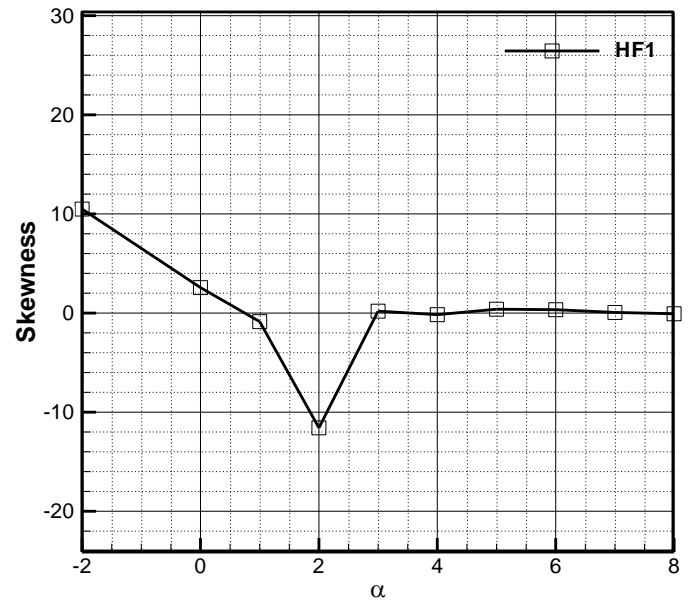


Figure 8c- Skewness graph $x/c=0.63$, $2y/b=0.34$, $\Lambda = 23^\circ$